Environment of hafnium and silicon in Hf-based dielectric films: An atomistic study by x-ray absorption spectroscopy and x-ray diffraction

J. Morais, L. Miotti, K. P. Bastos, S. R. Teixeira, I. J. R. Baumvol, A. L. P. Rotondaro, J. J. Chambers, M. R. Visokay, L. Colombo, and M. C. Martins Alves

---

Environment of hafnium and silicon in Hf-based dielectric films: An atomistic study by x-ray absorption spectroscopy and x-ray diffraction

J. Morais, L. Miotti, K. P. Bastos, and S. R. Teixeira
Instituto de Física, Universidade Federal do Rio Grande do Sul, Porto Alegre, 91501-970, Brazil

I. J. R. Baumvol
Centro de Ciências Exatas e Tecnológicas, Universidade de Caxias do Sul, Caxias do Sul, 95070-560, Brazil

A. L. P. Rotondaro, J. J. Chambers, M. R. Visokay, and L. Colombo
Silicon Technology Development, Texas Instruments Incorporated, Dallas, Texas, 75243

M. C. Martins Alves
Instituto de Química, Universidade Federal do Rio Grande do Sul, Porto Alegre, 91501-970, Brazil

The atomic structure of HfSiO and HfSiON was investigated before and after thermal annealing using x-ray diffraction and x-ray absorption spectroscopy. In HfSiO, the Hf atoms are arranged in a monoclinic HfO_2 structure with Hf as second nearest neighbors, while Si is in a SiO_2 environment. Thermal annealing induces crystallization of HfSiO with subtle changes in Hf–Hf distances. In the case of HfSiON, a stable structure is observed around the Hf atoms, which remains unaffected after annealing. Nitrogen is present in the first coordination shell of the Hf atoms, with Si in a SiON environment. © *2005 American Institute of Physics*. [DOI: 10.1063/1.1935042]

The aggressive scaling of complementary metal-oxide-semiconductor (CMOS) devices[1] has triggered a challenging search for a new material capable of replacing SiON as the gate dielectric in CMOS processing. Among the many materials that have been investigated, Hf-based dielectrics have been extensively studied[2–6] and are now considered for practical applications. However, there are some structural characteristics of HfO_2 and HfSiO that are not desirable. HfO_2 crystallizes at relatively low temperatures and even though HfSiO crystallizes at higher temperatures than HfO_2 depending upon the Si concentration, HfSiO exibits chemical phase separation at typical CMOS processing temperatures.[7,8] Recently, it was found that nitrogen incorporation into the HfSiO network to form HfSiON promotes phase stability, improved electrical performance, and reduced dopant diffusion.[3,9,10] The need remains, however, for a detailed atomic scale understanding of the fundamental issues concerning the atomistic origins of phase stability, as well as its evolution under thermal treatment, for both HfSiO and HfSiON dielectrics.

In this letter, a long-range order structural characterization by glancing incidence x-ray diffraction (XRD) is performed in conjunction with electronic and short-range order structural characterization provided by x-ray absorption spectroscopy (XAS). A combination of x-ray absorption near edge structure (XANES) and extended x-ray absorption fine structure (EXAFS) provides information on site geometry, degree of polyhedral distortion as well as bond distances and coordination numbers. The chemical environment around Hf and Si atoms in HfSiO and HfSiON dielectrics is described prior to and after 1000 °C annealing.

The films (~50 nm thick) were deposited by reactive sputtering onto 200 mm Si (100) wafers in a commercially available deposition system using a HfSi sputtering target. After deposition, the films were annealed using a lamp-based rapid thermal anneal chamber in nitrogen ambient (1 atm) at 1000 °C for 60 s. The composition of the as-deposited films was determined by channeled Rutherford backscattering spectroscopy and nuclear resonance analysis as $HfSi_{1.4}O_{3.6}$ and $HfSi_{1.4}O_{0.1}N_{2.6}$.

X-ray diffraction measurements were performed using an angle of incidence of the x-ray beam (Cu $K\alpha$ radiation) of 0.5° while the detector was swept to vary 2Θ.

X-ray absorption measurements at the Hf L_3 edge and Si K edge were performed at room temperature using XAS[11] and SXS[12] beam lines, respectively. The Hf L_3 edge XANES and EXAFS were measured in the fluorescence mode, while the Si K edge XANES were measured with total secondary electron yield detection using a dedicated UHV chamber. Hf XANES calculations were performed using the FEFF8 code.[13] Disorder effects were neglected in the FEFF calculation and the amplitude reduction factor (S_0^2) was set at 1.0.

The WINXAS program[14] was used for EXAFS data analysis. Structural parameters were obtained from a least squares fitting in the R space using theoretical phase shift and amplitude functions deduced from the FEFF code.

X-ray diffraction patterns obtained for the HfSiO and HfSiON samples before and after annealing, (data not shown), confirms that the HfSiO film is crystalline after annealing while the HfSiON film remains amorphous with the same thermal treatment.[10]

The comparison of XANES features at the Hf L_3 edge of the HfSiO film for the as-deposited and annealed sample [Fig. 1(a)] shows subtle modifications after thermal annealing. Both spectra display a strong resonance located at 9.56 keV (feature A) and a broad peak around 9.60 keV (feature C). These features correspond, respectively, to a dipole $2p \rightarrow 5d$ transition and the first EXAFS oscillation.[15] There are no detectable edge shifts among the spectra and the intensity of feature A remains the same after annealing. This is con-
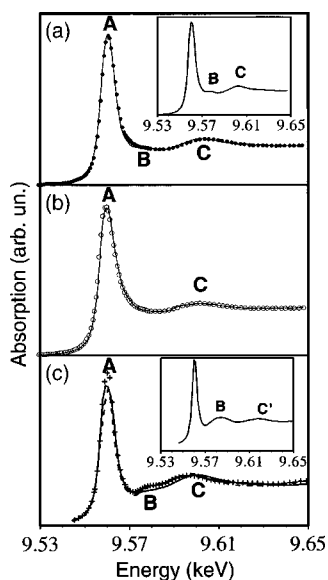
FIG. 1. Hf L_3 edge XANES spectra: (a) Comparison between HfSiO as deposited (full circle) and annealed in N_2 at 1000 °C for 60 s (solid line and inset); (b) comparison between HfSiON as deposited (○) and annealed in N_2 at 1000 °C for 60 s (—), (c) Hf L_3 edge XANES calculations for HfO_2 in the monoclinic (—), tetragonal (+), and cubic (–) structures. The inset shows the XANES calculation for tetragonal $HfSiO_4$ ("Hafnon").

FIG. 2. (a) Fourier Transform modulus of the EXAFS signals for as-deposited HfSiO (full circle) and annealed (dash–dot line); as deposited HfSiON (○) and annealed (—). Inset - k^1 weighted EXAFS signals: (i) as deposited HfSiO, (ii) annealed HfSiO, (iii) as deposited HfSiON, (iv) annealed HfSiON; (b) best fit obtained for the as-deposited HfSiO sample (modulus +imaginary part): experiment (full circle) and theory (solid lines).

sistent with the notion that the valency of Hf in these films remains the same and that a similar covalency prevails. The main differences observed in the spectra are related to the edge width, the presence of a small shoulder on the high energy side of the main resonance [feature B (see inset)], and a small shift to lower energy of feature C for the thermally treated sample. This modification of the XANES profile of the HfSiO films suggests that structural changes occurred within the film.

The XANES spectra of HfSiON films [Fig. 1(b)] for the as-deposited and annealed films are practically identical. The resonance peak A is weaker for the HfSiON films and the edge position is ≈1 eV lower when compared to the HfSiO films. These differences are associated with changes in the electronic structure of Hf ions, and indicate a lower density of Hf^{+4} ions in the HfSiON films.

To verify the origin of the XANES features at the Hf edge in Fig. 1(a) we have simulated three HfO_2 structures: monoclinic, tetragonal, and cubic. The calculations shown in Fig. 1(c) reproduced the strong resonance (feature A) and the broad peak (feature C) quite well. The small shoulder (feature B) is reproduced for HfO_2 in the tetragonal and cubic phases. Cluster size analysis revealed that feature B is a resonance originated in multiple scattering processes[12] corresponding to a collinear arrangement (Hf–O–Hf) including atoms located at the second neighboring shell. The calculation considering a tetragonal $HfSiO_4$ ("Hafnon") could not reproduce the experimental XANES features [see inset in Fig. 1(c)].

Fourier transforms (FT) of the EXAFS signals of the Hf K edge for HfSiO and HfSiON [Fig. 2(a)] allow us to compare their structural properties. The FT display two main peaks, the first one corresponds to the nearest neighbors around Hf and the second one to the next nearest neighbors. The main differences observed among FT of the HfSiO and HfSiON films are the intensity of the first peak related to the neighboring shell and the position of the next nearest neigh-
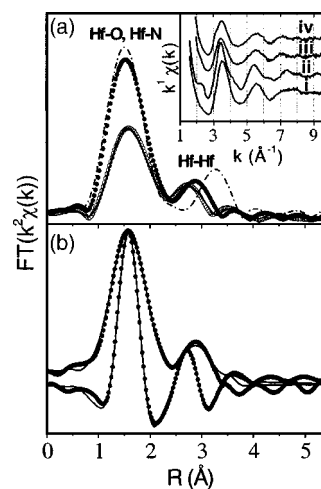
bors. The intensity of the peaks in the FT is dependent on the number and type of first neighbors and disorder, while their position depends on the distance. It is remarkable that the FT peaks of HfSiON display exactly the same pattern whose intensity and position remain unchanged after annealing.

The refinement of the data (Table I) was performed taking into account different possibilities. For the HfSiO film the first peak is easily assigned to a Hf–O contribution, however the nature of the second peak could be a Hf–Hf or a Hf–Si bond or a multiple scattering feature. The best fitting results were obtained considering oxygen as first neighbors and hafnium as second neighbors. For the best fit of the HfSiON, the first shell was simulated considering Hf–N and Hf–Hf contributions for the second shell. The lower amplitude of the FT peaks for the HfSiON is associated to the presence of N atoms at the first shell, since nitrogen is a weaker scatterer compared to oxygen. A good quality of fit is observed for the as-deposited HfSiO as shown in Fig. 2(b).

The results in Table I, obtained for the average bond distances, show that the Hf–O distance is the same for the as-deposited and annealed HfSiO sample, but the Hf–Hf distance is 0.25 Å longer for the latter. When comparing the HfSiO to the HfSiON samples, the most pronounced differences are related to Hf–Hf distances, which are shorter in the

TABLE I. Structural parameters related to the coordination and next nearest neighbors around Hf in the HfSiO and HfSiON films: Distance (R), number of neighbors (N), and the Debye Waller factor (σ^2).

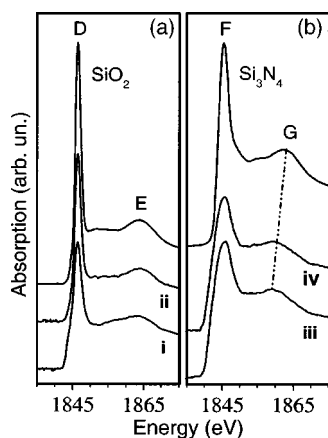|	R(Å)	Pair	N	σ^2(Å^2)
HfSiO as dep.	2.04±0.02	**(Hf–O)**	7.0±1.0	0.0138±0.002
	3.29±0.04	**(Hf–Hf)**	4.0±2.0	0.0113±0.004
HfSiO 1000 °C	2.06±0.02	**(Hf–O)**	7.6±1.0	0.0101±0.002
	3.54±0.04	**(Hf–Hf)**	6.4±2.0	0.0100±0.003
HfSiON as dep.	2.10±0.02	**(Hf–N)**	6.8±1.0	0.0140±0.002
	3.13±0.04	**(Hf–Hf)**	5.4±2.0	0.0144±0.004
HfSiON 1000 °C	2.10±0.02	**(Hf–N)**	6.8±1.0	0.0140±0.002
	3.13±0.04	**(Hf–Hf)**	5.4±2.0	0.0143±0.004

FIG. 3. (a) Si *K* edge XANES spectra for as-deposited (**i**), annealed HfSiO (**ii**), and a 50 nm thick SiO_2 film; (b) Si *K* edge XANES for as-deposited (**iii**), annealed HfSiON (**iv**), and a Si_3N_4 reference sample.

HfSiON. The number of first neighbors is around 7 for both HfSiO and HfSiON as-deposited films with a slight increase for the annealed HfSiO. This is in agreement with the previous report for Zr silicate systems with higher ZrO_2 content.[16] For annealed HfSiO the Hf–Hf distance corresponds to a cubic structure.[17]

Figure 3(a) displays the Si *K* edge XANES spectra for HfSiO samples discussed above and a SiO_2 film on Si as reference. All spectra exhibit strong resonance, located at 1846.5 eV labeled D, followed by a broad peak at around 1863.9 eV labeled E. These two features are characteristic of silicon's fourfold coordination to oxygen atoms.[18] After annealing, one notices an ordering effect since features D and E narrow down when compared to the as-deposited spectra. A comparison between the XANES spectra for HfSiON samples and a Si_3N_4 reference sample is shown in Fig. 3(b). Features F at 1845.6 eV and G at 1862.2 eV are observed in the Si_3N_4 reference sample. For HfSiON the feature F is broader while feature G appears at lower energy (1860.2 eV). These results suggest that the Si environment is similar to $Si_xO_yN_z$, presenting Si–O and Si–N bonds with higher degree of disorder, giving origin to the broader feature F. Our results show that the presence of N in the silicate network promotes thermal stability of the films and prevent crystallization upon annealing at 1000 °C.

The Hf XANES results and calculations suggest that Hf is present in monoclinic structure, in which Hf ions are in a distorted site, for all samples excluding the annealed HfSiO. Hafnium remains with a +4 oxidation state for the HfSiO films, however, in the case of HfSiON samples, its value is lower. The intensity[19] of the $2p \rightarrow 5d$ transition (feature A) depends on the filling of the *d* band, the Hf^{+4} ion has an empty 5d state ($5d^0 6s^0$) and Hf^{+3} is partially filled ($5d^1 6s^0$). This reduction in the oxidation state reinforces the existence of N in the first shell around Hf.

It was observed that N in the HfSiON network is present in the first shell of Hf and Si atoms, which is in agreement with recent work.[20] Simultaneously, Si atoms, in a silicon oxynitride bond state, acquire the beneficial properties of SiON. This association of bonds leads to a very stable struc-

ture. Our results are compatible with recent band structure calculations on the role of N in the structural stability of Hf-based dielectrics.[20]

In summary, XAS was used to untangle the environment of Hf and Si atoms in HfSiO and HfSiON films. For HfSiO, we observed that the Hf environment in annealed samples is very similar to HfO_2. Thermal annealing induces crystallization and changes to the next nearest neighbors' distances, with an increase of about 8% in the Hf–Hf distance when compared to the as-deposited HfSiO. The results confirm a $(HfO_2)_{1-x}(SiO_2)_x$ pseudobinary alloy description. The HfSiON system presents a stable amorphous structure at the atomic level, which remains unchanged upon annealing.

[1] *The International Technology Roadmap for Semiconductors* (Semiconductor Industry Association, 2003); http://public.itrs.net/
[2] J. Morais, L. Miotti, G. V. Soares, S. R. Teixeira, R. P. Pezzi, K. P. Bastos, I. J. R. Baumvol, A. L. P. Rotondaro, J. J. Chambers, M. R. Visokay, and L. Colombo, Appl. Phys. Lett. **81**, 1669 (2002).
[3] A. L. P. Rotondaro, M. R. Visokay, J. J. Chambers, A. Shanware, R. Khamankar, H. Bu, R. T. Laaksonen, L. Tsung, M. Douglas, R. Kuan, M. J. Bevan, T. Grider, J. McPherson, and L. Colombo, in *Symposium on VLSI Technology Digest of Technical Papers* (Honolulu, HI, 2002), pp. 148–149.
[4] M. Koyama, A. Kaneko, T. Ino, M. Koike, Y. Kamata, R. Iijima, Y. Kamimuta, A. Takashima, M. Suzuki, C. Hongo, S. Inumiya, M. Takayanagi, and A. Nishiyama, in *Technical Digest of IEEE International Electron Device Meeting* (2002), pp. 849–852.
[5] G. D. Wilk, R. M. Wallace, and J. M. Anthony, J. Appl. Phys. **89**, 5243 (2001).
[6] W. J. Qi, R. Nieh, E. Dharamarajan, B. H. Lee, Y. Jeon, L. Lang, K. Onishi, and J. C. Lee, Appl. Phys. Lett. **77**, 1704 (2000).
[7] D. A. Neumayer and E. Cartier, J. Appl. Phys. **90**, 1801 (2001).
[8] S. Stemmer, Z. Chen, C. G. Levi, P. S. Lysaght, B. Foran, J. A. Gisby, and J. R. Taylor, Jpn. J. Appl. Phys., Part 1 **42**, 3593 (2003).
[9] M. A. Quevedo-Lopez, M. El-Bouanani, B. E. Gnade, R. M. Wallace, M. R. Visokay, A. LiFatuo, M. J. Bevan, and L. Colombo, Appl. Phys. Lett. **81**, 1074 (2002).
[10] M. R. Visokay, J. J. Chambers, A. L. P. Rotondaro, A. Shanware, and L. Colombo, Appl. Phys. Lett. **80**, 3183 (2002).
[11] H. C. N. Tolentino, A. Y. Ramos, M. C. M. Alves, R. A. Barrea, E. Tamura, J. C. Cezar, and N. Watanabe, J. Synchrotron Radiat. **8**, 1040 (2001).
[12] H. C. N. Tolentino, V. Compagnon-Caillol, F. C. Vincentin, and M. Abbate, J. Synchrotron Radiat. **5**, 539 (1998).
[13] A. L. Ankudinov, B. Ravel, J. J. Rehr, and S. D. Conradson, Phys. Rev. B **58**, 7565 (1998).
[14] T. Ressler, J. Synchrotron Radiat. **5**, 118 (1998).
[15] M. Brown, R. E. Peierls, and E. A. Stern, Phys. Rev. B **15**, 738 (1977).
[16] G. Lucovsky and G. B. Raynor, Jr., Appl. Phys. Lett. **77**, 2912 (2000).
[17] A. S. Foster, F. L. Gejo, A. L. Shluger, and R. M. Nieminen, Phys. Rev. B **65**, 174117 (2002).
[18] D. Cabaret, M. L. Grand, A. Ramos, A.-M. Flank, S. Rossano, L. Galoisy, G. Calas, and D. Ghaleb, J. Non-Cryst. Solids **210**, 289 (2001).
[19] F. W. Lytle, P. S. P. Wei, R. B. Greegor, G. H. Via, and J. H. Sinfelt, J. Chem. Phys. **70**, 4849 (1979).
[20] M. S. Akbar, S. Gopalan, H.-J. Cho, K. Onishi, R. Choi, R. Nieh, C. S. Kang, Y. H. Kim, J. Han, S. Krishnan, and J. C. Lee, Appl. Phys. Lett. **82**, 1757 (2003).